

# Extending the range of real time density matrix renormalization group simulations



D.M. Kennes<sup>a</sup>, C. Karrasch<sup>b,c,\*</sup>

<sup>a</sup> Institut für Theorie der Statistischen Physik, RWTH Aachen University and JARA–Fundamentals of Future Information Technology, 52056 Aachen, Germany

<sup>b</sup> Department of Physics, University of California, Berkeley, CA 95720, USA

<sup>c</sup> Materials Sciences Division, Lawrence Berkeley National Laboratory, Berkeley, CA 94720, USA

## ARTICLE INFO

### Article history:

Received 13 June 2015

Received in revised form

5 September 2015

Accepted 28 October 2015

Available online 11 November 2015

### Keywords:

Density matrix renormalization group

Hints for beginners

Python code

## ABSTRACT

We discuss a few simple modifications to time-dependent density matrix renormalization group (DMRG) algorithms which allow to access larger time scales. We specifically aim at beginners and present practical aspects of how to implement these modifications within any standard matrix product state (MPS) based formulation of the method. Most importantly, we show how to ‘combine’ the Schrödinger and Heisenberg time evolutions of arbitrary pure states  $|\psi\rangle$  and operators  $A$  in the evaluation of  $\langle A \rangle_\psi(t) = \langle \psi | A(t) | \psi \rangle$ . This includes quantum quenches. The generalization to (non-)thermal mixed state dynamics  $\langle A \rangle_\rho(t) = \text{Tr}[\rho A(t)]$  induced by an initial density matrix  $\rho$  is straightforward. In the context of linear response (ground state or finite temperature  $T > 0$ ) correlation functions, one can extend the simulation time by a factor of two by ‘exploiting time translation invariance’, which is efficiently implementable within MPS DMRG. We present a simple analytic argument for why a recently-introduced disentangler succeeds in reducing the effort of time-dependent simulations at  $T > 0$ . Finally, we advocate the python programming language as an elegant option for beginners to set up a DMRG code.

© 2015 Elsevier B.V. All rights reserved.

## 1. Introduction

The density matrix renormalization group (DMRG) [1,2] was originally devised [3,4] as a tool to accurately determine *static* ground state properties of one dimensional systems. From a modern perspective, the core DMRG algorithm can be formulated elegantly if one introduces the concept of matrix product state (MPS) [5–8]. In principle, any given state of a 1d system can be expressed as a MPS:

$$|\psi\rangle = \sum_{\{\sigma_i\}} c_{\sigma_1 \dots \sigma_L} |\sigma_1 \sigma_2 \dots \sigma_L\rangle \stackrel{\text{SVD}}{=} \sum_{\{\sigma_i\}} M^{\sigma_1} \cdot M^{\sigma_2} \dots M^{\sigma_L} |\sigma_1 \sigma_2 \dots \sigma_L\rangle, \quad (1)$$

where  $\sigma_i$  denote single-particle quantum numbers (e.g.,  $\sigma_i = \uparrow, \downarrow$  for a spin-1/2 system). The mathematical algorithm which allows

to obtain the matrices  $M^{\sigma_i}$  from the coefficients  $c_{\sigma_1 \dots \sigma_L}$  is the so-called singular value decomposition (SVD). For an arbitrary 1d state, the dimension  $\chi$  of the matrices (which is often called bond dimension) grows exponentially with the size  $L$  of the system. The idea of a ground state DMRG calculation is to fix  $\chi$  to a value much smaller than  $e^L$  and to determine the matrices  $M^{\sigma_i}$  variationally. The reason why this is a reasonable approximation invokes the notion of entanglement. If one cuts the system and the amount of entanglement between left and right half is given by  $S$ , then the matrix at the cut site needs to be of dimension  $\chi \sim e^S$  to encode this. The entanglement, however, is not an extensive quantity,  $S \neq S(L)$ , but follows an area law—and the area between two 1d chains is a constant [9,10]. In other words, the ground state of one-dimensional systems<sup>1</sup> is entangled only locally, and this is perfectly coded by a MPS. Finally, the notion of a matrix product state can be generalized to operators so that all ‘ingredients’ for DMRG calculations are elegantly expressed using the same concepts [11–17]. One can show that each operator  $A$  can be recast as a

\* Corresponding author at: Department of Physics, University of California, Berkeley, CA 95720, USA. Tel.: +1 5106647052.

E-mail address: [c.karrasch@fu-berlin.de](mailto:c.karrasch@fu-berlin.de) (C. Karrasch).

<sup>1</sup> More precisely, of gapped 1d systems governed by local Hamiltonians.

matrix product operator (MPO)

$$A = \sum_{\{\sigma_i\}} \sum_{\{\tilde{\sigma}_i\}} A^{\sigma_1, \tilde{\sigma}_1} \cdot A^{\sigma_2, \tilde{\sigma}_2} \dots A^{\sigma_L, \tilde{\sigma}_L} |\{\sigma_i\}\rangle \langle \{\tilde{\sigma}_i\}| \quad (2)$$

if one again allows for an exponentially large bond dimension  $\chi \sim e^L$  [2]. Fortunately, most physical observables have a representation in terms of a MPO with a small  $\chi = O(1)$  that can be obtained by mere inspection; e.g. purely local operators  $A_i = \mathbb{1} \dots \mathbb{1} \cdot A_i \cdot \mathbb{1} \dots \mathbb{1}$  trivially are a MPO with  $\chi = 1$  (we will discuss a more complex example in Section 3.3).

*Time evolution*—Following the invention of the ground state DMRG [3,4], several algorithms were developed to simulate the real time evolution [18–23]. This allows to compute correlation functions  $\langle \text{gs} | A(t) B | \text{gs} \rangle^2$  or to calculate the evolution of observables  $\langle \psi | A(t) | \psi \rangle$  in arbitrary initial states. One of the most common approaches is the so-called time-dependent DMRG, which can be formulated very elegantly using matrix product states. Its basic idea is to split up the time evolution into small steps,  $\exp(-iHt) = \exp(-iH\Delta t) \exp(-iH\Delta t) \dots$  and to Trotter-decompose [32] the exponentials via  $\exp(-iH\Delta t) = \exp(-i\tilde{h}_a\Delta t) \exp(-i\tilde{h}_b\Delta t) + O([\Delta t]^2)^3$  into factors which only contain local, mutually commuting terms  $\tilde{h}_{a,b}$  such as nearest-neighbor Heisenberg spin interactions  $\tilde{S}_1 \tilde{S}_2$ . Local terms, however, can be applied straightforwardly to a MPS—they act only on the matrices living at the corresponding sites, e.g.:

$$M^{\sigma_1}, M^{\sigma_2} \xrightarrow{\exp(-i\tilde{S}_1 \tilde{S}_2 \Delta t)} f(M^{\sigma_1}, M^{\sigma_2}) \xrightarrow{\text{SVD}} \tilde{M}^{\sigma_1}, \tilde{M}^{\sigma_2}. \quad (3)$$

The main tool to bring the resulting state back to the form of a MPS is again the singular value decomposition. The algorithm is explained in great detail in the literature [2] and will also be made more explicit in Section 4.

In order to approximate  $\langle \text{gs} | A(t) B | \text{gs} \rangle$  or  $\langle \psi | A(t) | \psi \rangle$  to a certain accuracy, the dimension of the matrix product state needs to be increased with time, often even exponentially. Physically, this is due to the buildup of entanglement in the system, and it limits the accessible time scales. Modified algorithms such as transverse folding [33] hold the promise of substantially extending the range of simulations, but implementing them in practice requires some effort (for a comprehensive overview of other available approaches see Ref. [2] and references therein). It is one of the goals of this paper to discuss a few *simple* ‘recipes’ that allow to reach larger times in DMRG calculations. In particular, we will investigate if the Schrödinger and Heisenberg pictures of quantum mechanics can be combined efficiently.

*Finite temperatures*—Standard DMRG methods allow computing the time evolution of a *pure* state and are thus not directly applicable at finite temperatures. In order to simulate dynamics at  $T > 0$ , one can use operator space DMRG [34,35], or – equivalent mathematically – one can express the thermal statistical operator  $\rho_T \sim e^{-H/T}$  as a partial trace over a pure state  $|\Psi_T\rangle$  living in an enlarged Hilbert space where auxiliary degrees of freedom  $Q$  encode the thermal bath [36–40]<sup>4</sup>:

$$\rho_T = \text{Tr}_Q |\Psi_T\rangle \langle \Psi_T|. \quad (4)$$

A finite- $T$  correlation function can in principle be obtained straightforwardly by carrying out real- and imaginary time evolutions of the state  $|\psi_\infty\rangle$  which purifies  $\rho_T$  at  $T = \infty$  [2]:

$$C_T^{AB}(t) = \text{Tr} [\rho_T A(t) B] \\ = \langle \Psi_T | A(t) B | \Psi_T \rangle \sim \langle \psi_\infty | e^{-H/2T} A(t) B e^{-H/2T} | \psi_\infty \rangle. \quad (5)$$

Since  $\rho_\infty \sim 1$ , the state  $|\psi_\infty\rangle$  is known; it is given by a product of local states, which for a spin-1/2 system read  $|\psi_\infty\rangle \sim |\uparrow \downarrow_Q\rangle - |\downarrow \uparrow_Q\rangle$ . It is another goal of this paper to recapitulate recent ideas [40, 34] of how to extend the range of real-time DMRG simulation at finite temperature in a didactic way.

*Structure of the paper*—We will discuss a few *simple* ‘recipes’ that allow to reach larger times in DMRG calculations. The combination of the Schrödinger and Heisenberg pictures is investigated in Section 2. Prior ideas of how to extend the range of finite temperature calculations are presented in a didactical way in Section 3. We specifically aim at an audience of beginners and ask: Assuming that one has a standard MPS based DMRG code at hand, what are the most important practical steps necessary to incorporate these recipes? We will particularly elaborate how to incorporate Abelian symmetries [48]. For colleagues new to the realm of DMRG, we try to advocate the method in general by showing how straightforwardly its core algorithms can be implemented within the python programming language (Section 4). Throughout this paper, we perform our DMRG calculations using a fixed small discarded weight and a 4th order Trotter decomposition of the time evolution operators.

## 2. Schrödinger vs. Heisenberg picture

### 2.1. General aspects

Let us assume we want to compute the time evolution of an observable  $A$  in a given state  $|\psi\rangle$ ,

$$\langle A \rangle_\psi(t) = \langle \psi | A(t) | \psi \rangle, \quad (6)$$

or similarly at finite temperature by enlarging the Hilbert space and choosing  $|\psi\rangle$  as the state which purifies the initial density matrix,  $\langle A \rangle_\rho(t) = \text{Tr} [\rho A(t)] = \langle \psi_\rho | A(t) | \psi_\rho \rangle$ . The most straightforward way to evaluate Eq. (6) within DMRG is to simulate  $e^{-iHt} |\psi\rangle$ . This corresponds to a time evolution in the Schrödinger picture. If one expresses  $A$  as a matrix product operator, one can alternatively switch to the Heisenberg picture and calculate the operator time evolution  $e^{iHt} A e^{-iHt}$  [11–13, 48, 14–17]. This is equivalent mathematically but different algorithmically since  $e^{iHt} A e^{-iHt}$  might have a more efficient representation in terms of a MPO than  $e^{-iHt} |\psi\rangle$  has in terms of a MPS (or vice versa). For example, the Schrödinger picture is certainly advantageous whenever  $|\psi\rangle$  is close to an eigenstate of  $H$ . Of course, it is possible to simply split the time evolution between the Schrödinger- and Heisenberg picture,

$$\langle A \rangle_\psi(2t) = \langle \psi | e^{iHt} A(t) e^{-iHt} | \psi \rangle, \quad (7)$$

and evaluate  $e^{-iHt} |\psi\rangle$  as well as  $A(t)$  individually. Generally speaking, if one stops each simulation at times  $t_\psi$  and  $t_A$  where a fixed bond dimension is reached, one can *always* reach larger time scales  $t_\psi + t_A > t_\psi, t_A$ .<sup>5</sup> In practice, however,  $t_\psi$  might be significantly smaller than  $t_A$  or vice versa, and the additional effort to implement Eq. (7) might simply not be justified. We will now discuss this using an instructive example.

### 2.2. Examples

We consider the time evolution of a local spin operator  $S_i^z$  under the XXZ spin chain Hamiltonian:

$$H = \sum_{l=1}^{L-1} \left[ \frac{1}{2} (S_l^+ S_{l+1}^- + S_l^- S_{l+1}^+) + \Delta S_l^z S_{l+1}^z \right] + b \sum_{l=1}^L S_l^z, \quad (8)$$

<sup>2</sup> For other approaches to calculate correlation functions, see Refs. [1, 24–31].

<sup>3</sup> In practice, higher-order approximations are used; see, e.g., Ref. [2].

<sup>4</sup> Various other ways to incorporate finite temperatures within DMRG, e.g., using minimally entangled typical thermal states [41], can be found in Refs. [42–47].

<sup>5</sup> This is not hindered by a more costly ‘overlap’ calculation; see Section 2.3 for details.

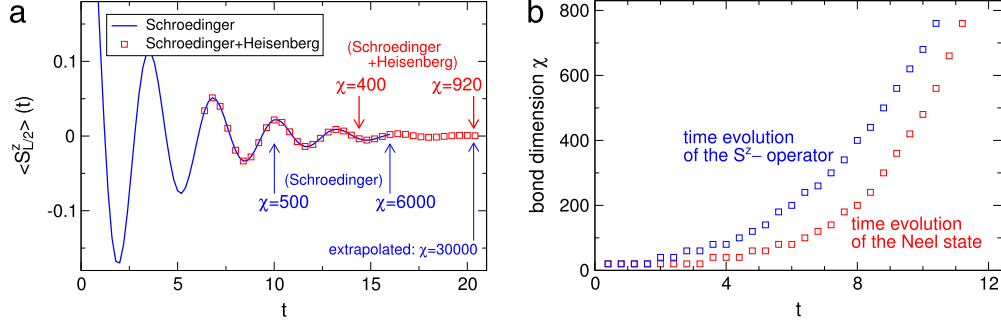


**Fig. 1.** (Color online) (a) DMRG calculation of the spin expectation value  $\langle S_{L/2}^z \rangle_{\text{NS}}(t) = \langle \text{NS} | S_{L/2}^z(t) | \text{NS} \rangle$  in a Neel state  $|\text{NS}\rangle$  under the XXZ Hamiltonian of Eq. (8) with  $\Delta = 0.5, b = 0$ , and  $L = 100$ . If the time evolution is split equally between the Schrödinger and Heisenberg pictures via Eq. (7), the simulation can be pushed to larger times with no additional effort. (b) Growth of the bond dimension  $\chi$  during the evaluation of  $e^{-iHt}|\text{NS}\rangle$  and  $S_{L/2}^z(t)$ . Note that the latter can be computed straightforwardly within any existing MPS based implementation of the method (see Section 2.3 for details).

where  $S^\pm = S^x \pm iS^y$ , and  $S^{x,y,z}$  are spin-1/2 operators. In [12], it was shown that  $S_i^z(t)$  can be expressed exactly in terms of a MPO with a finite bond dimension if  $\Delta = 0$ ; hence, the time evolution  $\langle A = S_i^z \rangle_\psi(t)$  can be simulated up to arbitrary long times for any state  $|\psi\rangle$  using the Heisenberg picture. The same certainly holds also for any  $A$  and  $\Delta \neq 0$  if  $|\psi\rangle$  is an eigenstate of  $H$  using the Schrödinger picture. For a general scenario in between those two extreme limits, however, one would expect that the bond dimension  $\chi$  increases equally fast during the calculation of  $e^{-iHt}|\psi\rangle$  and  $e^{iHt}Ae^{-iHt}$ . As a concrete example, we investigate the time evolution of  $S_i^z$  in a Neel state  $|\text{NS}\rangle$ . We know that  $\langle S_i^z \rangle_{\text{NS}}$  can be computed trivially (1) in the Schrödinger picture for  $\Delta = \infty$ , or (2) in the Heisenberg picture for  $\Delta = 0$ . For a generic value of  $\Delta = O(1)$ , however, the bond dimension grows equally fast during the evaluation of  $e^{-iHt}|\text{NS}\rangle$  and  $S_i^z(t)$ . This is shown in Fig. 1(a,b) for  $\Delta = 0.5$  (results for  $\Delta = 0.25$  and  $\Delta = 1$  look similar). Combining the Schrödinger and Heisenberg picture thus allows to access time scales roughly twice as large [see Fig. 1(a)] using the same  $\chi$ . Since  $\chi$  typically grows exponentially fast (by extrapolation one can estimate the bond dimension required to reach  $t \sim 20$  within the Schrödinger picture to be  $\chi \sim 30,000$ ), this amounts to major algorithmic savings.

As a second example, we study a *local quench* at finite temperature described by an initial density matrix  $\rho = \rho_L^L \otimes \rho_{\uparrow\uparrow\uparrow\uparrow} \otimes \rho_R^R$ . This models a wave packet of four up-spins surrounded to its left and right by chains in thermal equilibrium. We focus on the isotropic XXZ chain ( $\Delta = 1$ ) and compute the time evolution of  $S_i^z$  via

$$\langle S_i^z \rangle_\rho(t) = \text{Tr}[\rho e^{iHt} S_i^z e^{-iHt}] = \langle \psi_\rho | e^{iHt} S_i^z e^{-iHt} | \psi_\rho \rangle, \quad (9)$$

$$\rho = \text{Tr}_Q |\psi_\rho\rangle \langle \psi_\rho|,$$

where the state  $|\psi_\rho\rangle$  which purifies  $\rho$  can be obtained straightforwardly from  $|\psi_T\rangle$  and the trivial purification of  $\rho_{\uparrow\uparrow\uparrow\uparrow}$ . We separately calculate  $e^{-iHt} e^{iH_Q t} |\psi_\rho\rangle$ , where we insert  $e^{iH_Q t}$  to reduce the buildup of entanglement (see the discussion in Section 3), as well as  $S_i^z(t)$ . As illustrated in Fig. 2, the bond dimension grows comparably fast during both simulations, and thus larger time scales can be reached if they are combined. Note that the ‘standard’ approach (e.g., used in Ref. [49]) is to time-evolve only the state  $|\psi_\rho\rangle$  but not  $S_i^z$ .

### 2.3. Practical detail: Operator time evolution within MPS DMRG

In this section, which solely aims at DMRG beginners, we discuss a few practical aspects of how to simulate the operator time evolution  $A(t)$  [11–13,48,14–17] using an existing MPS based DMRG implementation. Put differently: We want to provide a simple practical guide of how to calculate  $A(t)$  assuming that one

has a standard DMRG code at hand which allows to compute the time evolution of a state.

We will now discuss two alternative approaches of how to simulate  $A(t)$  provided that the MPO representation of  $A$  is known. In particular, we will illustrate that Abelian symmetries can be exploited straightforwardly; it is thus instructive to recapitulate how such symmetries are generally incorporated within DMRG numerics (we follow Ref. [2]). To this end, let us consider an eigenstate  $|\psi\rangle$  of an operator  $M = \sum M_l$  which defines an additive local quantum number,  $M_l|\sigma_l\rangle = m(\sigma_l)|\sigma_l\rangle$ . One can show recursively that  $|\psi\rangle$  can be expressed as a MPS whose ‘block states’

$$|a_l\rangle = \sum_{\{\sigma_i\}} (M^{\sigma_1} \cdots M^{\sigma_l})_{1,a_l} |\{\sigma_i\}\rangle \quad (10)$$

are eigenstates of  $\sum_{l \leq l_0} M_l$  with a quantum number of  $m_l^\Sigma$ ; this implies that all matrix elements in Eq. (1) vanish except for those with

$$m_l^\Sigma + m(\sigma_{l+1}) = m_{l+1}^\Sigma, \quad (11)$$

and the same obviously holds for the time-evolved state  $e^{-iHt}|\psi\rangle$  if  $[H, M] = 0$ . Eq. (11) can be readily incorporated within a DMRG code<sup>6</sup> to significantly reduce the computational effort—for the problems studied in this work, numerics speed up by a factor of 10 for a bond dimension of  $\chi \sim 1000$ . If the model at hand features more than one Abelian symmetry, this can be exploited within any existing code without having to modify it at all. For example, in case of the Fermi–Hubbard model

$$H = \sum_l \left\{ - \sum_\sigma \left[ \frac{1}{2} c_{l\sigma}^\dagger c_{l+1\sigma} + \text{h.c.} \right] + U n_{l\uparrow} n_{l\downarrow} + \mu (n_{l\uparrow} + n_{l\downarrow}) + b (n_{l\uparrow} - n_{l\downarrow}) \right\}, \quad n_{l\sigma} = c_{l\sigma}^\dagger c_{l\sigma} - \frac{1}{2}, \quad (12)$$

where both the total spin and charge are conserved, one simply assigns the following quantum numbers to the states  $\{|0\rangle, |\uparrow\rangle, |\downarrow\rangle, |\uparrow\downarrow\rangle\}$  which span its local Hilbert space:

$$m(0) = 0, \quad m(\uparrow) = 1, \quad m(\downarrow) = M_0, \quad (13)$$

$$m(\uparrow\downarrow) = M_0 + 1,$$

where  $M_0 > 2L$  is an arbitrary integer. This automatically accounts for both spin and charge conservation ( $M_0 > 2L$  guarantees the separation of the two symmetries). Other models/symmetries can be treated analogously.

<sup>6</sup> While exploiting Abelian symmetries within the MPS numerics is straightforward, incorporating continuous non-Abelian symmetries is much more involved [50–52].

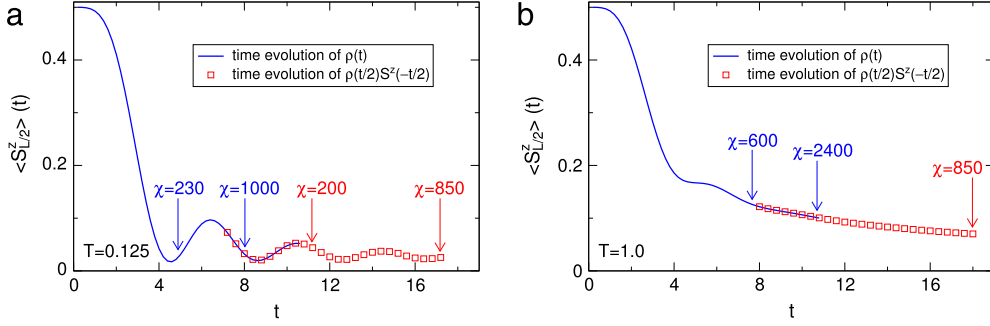


**Fig. 2.** (Color online) Spin expectation value  $\langle S_{L/2}^z \rangle_\rho(t)$  following a local quench at finite temperatures. At time  $t = 0$ , a ‘wave packet’ of four up-spins is prepared at the center of an isotropic XXZ chain ( $\Delta = 1$ ,  $b = 0$ ) of length  $L = 100$  which is otherwise in thermal equilibrium. This initial geometry is described by a density matrix  $\rho = \rho_T^L \otimes \rho_{\uparrow\uparrow\uparrow\uparrow} \otimes \rho_T^R$ . One can calculate  $\langle S_i^z \rangle_\rho(t) = \text{Tr}[\rho e^{iHt} S_i^z e^{-iHt}]$  either by a straightforward time evolution of the state which purifies  $\rho$  [49], or using  $\langle S_i^z \rangle_\rho(t) = \text{Tr}[\rho(-t/2) S_i^z(t/2)]$  and time-evolving  $\rho(-t/2)$  as well as  $S_i^z(t/2)$  separately. The latter allows to perform the simulation up to larger times.

*The trivial way*—The coefficients  $A^{\sigma_1, \tilde{\sigma}_1} \dots A^{\sigma_L, \tilde{\sigma}_L}$  appearing in Eq. (2) are nothing but the coefficients of a matrix product state whose local Hilbert space is  $d^2$ -dimensional and parametrized by a superindex  $\Sigma_l = (\sigma_l, \tilde{\sigma}_l)$ . The time evolution operators  $e^{iHt}$  (acting on  $\sigma_l$ ) as well as  $e^{-iHt}$  (acting on  $\tilde{\sigma}_l$ ) can thus be applied directly using an existing MPS based DMRG code [48]. The only (minor) subtlety is how to incorporate Abelian symmetries (in case that the initial  $A$  respects them) to speed up the calculation. If  $M = \sum_l M_l$  is conserved, this can be exploited by assigning a quantum number  $m(\sigma, \tilde{\sigma}) = m(\sigma) - m(\tilde{\sigma})$  to the local states  $\{|\sigma, \tilde{\sigma}\rangle\}$  within the MPS numerics; for a spin-1/2 system ( $d = 2$ ) and  $M = S^z$ , the  $m$ ’s read

$$\begin{aligned} m(\Sigma = \uparrow\uparrow) &= 0, & m(\Sigma = \downarrow\downarrow) &= 0, \\ m(\Sigma = \uparrow\downarrow) &= 1, & m(\Sigma = \downarrow\uparrow) &= -1. \end{aligned} \quad (14)$$

Other symmetries follow analogously. The computational effort of this approach scales as  $d^6 \chi^3$  [2].

*Employing finite- $T$  numerics*—For models with a large local Hilbert space dimension (such as the Hubbard model where  $d = 4$ ) one can resort to an alternative approach. After recasting the coefficients in Eq. (2) via a singular value decomposition,

$$\begin{aligned} [A^{\sigma_l, \tilde{\sigma}_l}]_{a_l, \tilde{a}_{l+1}} &= A_{(a_l \sigma_l), (a_{l+1} \tilde{\sigma}_l)} \stackrel{\text{SVD}}{=} \sum_{s_l} U_{(a_l \sigma_l), s_l} S_{s_l} V_{s_l, (a_{l+1} \tilde{\sigma}_l)} \\ &= \sum_{s_l} [M^{\sigma_l}]_{a_l, s_l} [\tilde{M}^{\tilde{\sigma}_l}]_{s_l, a_{l+1}}, \end{aligned} \quad (15)$$

the (appropriately normalized) matrices  $M = U$  and  $\tilde{M} = SV$  define a MPS whose local Hilbert space dimension is reduced back to  $d$ . However,  $M^{\sigma_l}$  and  $M^{\sigma_{l+1}}$  are now next-nearest neighbors, and  $e^{iHt}$  therefore contains longer-ranged interactions (the same holds for  $e^{-iHt}$  which couples the  $\tilde{M}$ ). Computing the time evolution  $A(t)$  is thus just as easy (or hard) as it is to simulate dynamics at finite temperatures (note that now *all sites* are physical ones). One can exploit  $S^z$ -conservation (or any other Abelian symmetry) by simply performing a spin-flip transformation  $\tilde{\uparrow} \rightarrow \tilde{\downarrow}$ , which then allows to straightforwardly employ the usual quantum numbers  $m(\sigma) = \sigma$ ,  $m(\tilde{\sigma}) = \tilde{\sigma}$ . The numerical cost to carry out the time evolution  $A(t)$  scales as  $d^4 \chi^3$ .

It seems instructive to illustrate the algorithmic simplicity of the second approach for two concrete examples: In order to calculate  $S_i^z(t)$  or the potential energy  $E_K = -L[S_i^z S_{i+1}^z](t)/\Delta$  for a Heisenberg chain, one needs to time-evolve the states

$$\begin{aligned} |\psi_{S^z}\rangle &= |\psi_{\uparrow}\rangle \otimes \dots \otimes |\psi_{\uparrow}\rangle \otimes |\psi_{S^z+1/2}\rangle \otimes |\psi_{\uparrow}\rangle \otimes \dots \otimes |\psi_{\uparrow}\rangle, \\ |\psi_{E_K}\rangle &= |\psi_{\uparrow}\rangle \otimes \dots \otimes |\psi_{\uparrow}\rangle \otimes |\psi_{S^z+1/2}\rangle \otimes |\psi_{S^z+1/2}\rangle \otimes |\psi_{\uparrow}\rangle \\ &\quad \otimes \dots \otimes |\psi_{\uparrow}\rangle, \\ |\psi_{\uparrow}\rangle &= |\uparrow\rangle |\tilde{\downarrow}\rangle + |\downarrow\rangle |\tilde{\uparrow}\rangle, & |\psi_{S^z+1/2}\rangle &= |\uparrow\rangle |\tilde{\downarrow}\rangle \end{aligned} \quad (16)$$

under  $e^{\pm iHt}$  which now contain purely next-nearest neighbor interactions between either only odd or even sites. This is almost completely equivalent to simulating a time evolution  $e^{-iHt} |\psi_T\rangle$  at finite temperature and can thus be achieved directly with any code that can access  $T > 0$  dynamics.

While carrying out the time evolution scales as  $\chi^3$  in both approaches, computing  $\langle \psi | e^{iHt} A(t) e^{-iHt} | \psi \rangle$  requires an overlap calculation which scales as  $d^2 \chi^4$ . Thus, the latter will eventually dominate the numerical effort and render it impossible to combine the Schrödinger and Heisenberg pictures. As already illustrated by Figs. 1 and 2 (whose data was obtained with minor effort), this is not the case in most practical applications. The reason for this pragmatic observation is two-fold: First, computing an overlap involves matrix multiplications, which are *significantly* faster than carrying out a singular value decomposition (the bottleneck in the time evolution algorithms), even if one employs a SVD routine from highly optimized libraries such as Intel’s Math Kernel Library. Moreover, the overlap calculation is highly parallelizable and scales much better with the number of low-level threads (typically 20 in our case) than the SVD for bond dimensions that occur in practice. Second, the additional factor of  $\chi$  needs to be compared to the (typically) much faster growth of  $\chi$  due to the buildup of entanglement: computing  $S^z(t)$  in Fig. 1(a) up to times  $t \sim 20$  within the Schrödinger picture would require a bond dimension of roughly  $\chi \sim 30,000$  as opposed to  $\chi \sim 900$  if both pictures are combined.

### 3. Finite-temperature dynamics

#### 3.1. General aspects

As explained in the introduction, finite temperatures can be incorporated within the DMRG by enlarging the Hilbert space. The time scales accessible within those straightforward finite- $T$  calculations were, however, considerably smaller than those reached at  $T = 0$  [38]. In Refs. [40,53] it was then shown that one can exploit the fact that purification is not unique to push simulations to larger times.<sup>7</sup> In particular, one can insert any unitary transformation  $U_Q(t) : Q \rightarrow Q$  which solely acts on the auxiliary Hilbert space  $Q$  into Eq. (5):

$$\begin{aligned} \rho_T &= \text{Tr}_Q |\Psi_T\rangle \langle \Psi_T| = \text{Tr}_Q U_Q(t) |\Psi_T\rangle \langle \Psi_T| U_Q^\dagger(t), \\ &\Rightarrow C_T^{AB}(t) = \langle \Psi_T | U_Q^\dagger(t) A(t) U_Q(t) B | \Psi_T \rangle. \end{aligned} \quad (17)$$

<sup>7</sup> An alternative approach to potentially extend the range of simulations substantially is the probabilistic sampling over an appropriately chosen set of pure states introduced in Ref. [41].

It turned out that choosing  $U_Q(t) = e^{iH_Q t}$ , i.e. a time evolution in  $Q$  governed by the physical Hamiltonian (where physical degrees of freedom are replaced by auxiliary ones) but reversed time leads to a slower increase of the bond dimension, and thus longer time scales can be reached (a systematic way to further optimize  $U_Q(t)$  was introduced in Refs. [34,35]; particularly at low temperatures, this allows to access larger times). In the realm of Ref. [40], however, the specific form of  $U_Q(t) = e^{iH_Q t}$  was nothing but a ‘lucky guess’. Eq. (17) was subsequently mapped to a problem of time-evolving operators [34], which then provided an understanding of the ‘disentangler’  $U_Q(t)$ . Moreover, the backward time evolution of the auxiliary degrees of freedom very naturally emerges in a Liouville space formulation [54,55,31]. While mathematically equivalent, we aim at reformulating the argument of Ref. [34] in the *simplest possible* way for didactic purposes. More importantly, this yields an explanation for why the signs of certain terms in  $H_Q$  need to be reversed (and provides a strategy to determine which ones) if symmetries are exploited in the MPS formalism.

### 3.2. Didactic explanation of the disentangler

For didactic reasons, we will now give the simplest possible (yet missed in Ref. [40]) analytic argument for why the particular choice  $U_Q(t) = e^{iH_Q t}$  – i.e., evolving  $Q$  backwards in time with the physical Hamiltonian  $H_Q$  acting on the auxiliary degrees of freedom – succeeds in reducing the growth of entanglement. We present a straightforward way to determine whether or not the sign of any terms in  $H_Q$  needs to be flipped if for a given model Abelian symmetries are incorporated within the MPS numerics.

Let us begin with the Heisenberg chain defined in Eq. (8) and try to analytically understand the time evolution of the state  $|\psi_T\rangle$  which purifies the density matrix. Since  $|\psi_T\rangle \sim e^{-H/T}|\psi_\infty\rangle$  and  $H$  commutes with  $H_Q$ , it is sufficient to study  $e^{-iHt}e^{iH_Q t}|\psi_\infty\rangle$ . Starting from Ref. [2], we need to choose  $|\psi_\infty\rangle$  as follows in order to exploit the conservation of the total (physical plus auxiliary) spin:

$$|\psi_\infty\rangle = \bigotimes_{l=1}^L |\psi_{\infty,l}\rangle, \quad |\psi_{\infty,l}\rangle = \frac{1}{\sqrt{2}}(|\uparrow_l\downarrow_{l,Q}\rangle - |\downarrow_l\uparrow_{l,Q}\rangle), \quad (18)$$

where we have combined physical and auxiliary degrees of freedom  $\sigma_l$  and  $\sigma_{l,Q}$  to a single site whose Hilbert space is spanned by  $\{|\uparrow\uparrow\rangle, |\uparrow\downarrow\rangle, |\downarrow\uparrow\rangle, |\downarrow\downarrow\rangle\}$ . Applying  $H \otimes \mathbb{1}$  then induces the following transitions between neighboring sites:

$$\begin{aligned} \downarrow\uparrow | \uparrow\downarrow &\xrightarrow{(1/2)(S^+ \otimes \mathbb{1}) \otimes (S^- \otimes \mathbb{1})} (1/2) \uparrow\uparrow | \downarrow\downarrow \\ \uparrow\downarrow | \downarrow\uparrow &\xrightarrow{(1/2)(S^- \otimes \mathbb{1}) \otimes (S^+ \otimes \mathbb{1})} (1/2) \downarrow\downarrow | \uparrow\uparrow \\ x|y &\xrightarrow{(\Delta)(S^z \otimes \mathbb{1}) \otimes (S^z \otimes \mathbb{1})} \text{sign}_1(x)\text{sign}_1(y)(\Delta/4)x|y \\ x|y &\xrightarrow{(b)(S^z \otimes \mathbb{1}) \otimes (\mathbb{1} \otimes S^z)} (b/2)\text{sign}_1(x)x|y, \end{aligned} \quad (19)$$

where  $x, y \in \{\uparrow\downarrow, \downarrow\uparrow\}$ ,  $\text{sign}_1(\uparrow\downarrow) = 1$ , and  $\text{sign}_1(\downarrow\uparrow) = -1$ . The time evolution of  $|\psi_\infty\rangle$  governed by  $H \otimes \mathbb{1}$  is thus non-trivial; entanglement starts to build up. However, applying  $-\mathbb{1} \otimes H_Q$  induces the same transitions but with opposite sign and hence undoes this damage:

$$\begin{aligned} \downarrow\uparrow | \uparrow\downarrow &\xrightarrow{(-1/2)(\mathbb{1} \otimes S^-) \otimes (\mathbb{1} \otimes S^+)} (-1/2) \downarrow\downarrow | \uparrow\uparrow \\ \uparrow\downarrow | \downarrow\uparrow &\xrightarrow{(-1/2)(\mathbb{1} \otimes S^+) \otimes (\mathbb{1} \otimes S^-)} (-1/2) \uparrow\uparrow | \downarrow\downarrow \\ x|y &\xrightarrow{(-\Delta)(\mathbb{1} \otimes S^z) \otimes (\mathbb{1} \otimes S^z)} [-\text{sign}_1(x)][-\text{sign}_1(y)](-\Delta/4)x|y \\ x|y &\xrightarrow{(b)(\mathbb{1} \otimes S^z) \otimes (\mathbb{1} \otimes \mathbb{1})} (b/2)[- \text{sign}_1(x)]x|y, \end{aligned} \quad (20)$$

if additionally the sign of the magnetic field  $b$  is reversed in  $H_Q$ . The total time evolution governed by  $H \otimes \mathbb{1} - \mathbb{1} \otimes H_Q$  therefore

becomes trivial, or put differently: While  $|\psi_\infty\rangle$  is not an eigenstate of  $H$  alone, it is an eigenstate of  $H - H_Q$  (and the same holds for  $|\psi_T\rangle$ ). The calculation of  $A(t)|\psi_T\rangle$  is therefore only plagued by an entanglement building up around the region where  $A$  acts (the physical reason being quasi-locality [34,35]). This simple fact, which was missed in Ref. [40], explains why the particular choice  $U_Q(t) = e^{iH_Q t}$  reduces the growth of entanglement during calculations at finite temperature (see also Ref. [34]). The Hubbard model defined in Eq. (12) can be analyzed analogously, and it turns out that if  $|\psi_\infty\rangle$  is chosen such that one can exploit the conservation of both the total spin and the total charge, the signs of  $\mu$  and  $b$  need to be reversed in  $H_Q$ .

### 3.3. A factor of two

To the best of our knowledge, it was overlooked for a long time (and only recently noticed in Ref. [34] in an implicit way in the specific context of optimizing calculations at  $T > 0$ ) that one can simply ‘exploit time translation invariance’ in linear response correlation functions to extend the range of simulations by a factor of two:

$$\begin{aligned} C_{\text{gs}}^{AB}(2t) &= \langle \text{gs} | A(t)B(-t) | \text{gs} \rangle, \\ C_T^{AB}(2t) &= \text{Tr}[\rho_T A(t)B(-t)] = \langle \psi_T | A(t)B(-t) | \psi_T \rangle. \end{aligned} \quad (21)$$

At  $T = 0$  one needs to carry out two individual calculations for  $e^{iHt}A|\text{gs}\rangle$  as well as  $e^{-iHt}B|\text{gs}\rangle$ , which can be done straightforwardly using MPS DMRG (at least if  $A$  and  $B$  are local operators; we will come back to this below). At  $T > 0$ , however, the forward and backward time evolutions in  $e^{iHt_n}Ae^{-iHt_n}|\psi_T\rangle$  need to be carried out individually for each  $t_n$  in order to obtain  $\langle \psi_T | A(t_n)B(-t_n) | \psi_T \rangle$  for all  $t_n \in [0, t]$  (and likewise for  $B$ ), which is possible [56] but costly. However, given the ‘insights’ of the previous section that  $|\psi_T\rangle$  is an eigenstate of  $H - H_Q$ , we can recast Eq. (21) as

$$\begin{aligned} C_T^{AB}(2t) &= \langle \psi_T | e^{iHt} A e^{-iHt} e^{-iHt} B e^{-iHt} | \psi_T \rangle \\ &= \langle \psi_T | A e^{-iHt+iH_Q t} e^{-iHt+iH_Q t} B | \psi_T \rangle, \end{aligned} \quad (22)$$

and are left with the significantly simpler task to calculate  $e^{-iHt+iH_Q t}A|\psi_T\rangle$  (as well as  $e^{iHt-iH_Q t}B|\psi_T\rangle$ ) via a single DMRG simulation up to the time  $t$ . Note that the ‘disentangler’  $U_Q(t)$  is automatically included in Eq. (22).

In case that  $A$  is given by a product of local operators (e.g.,  $S_i^z$  or  $S_{i+1}^+ S_i^-$ ), it can be applied straightforwardly to a MPS representation of  $|\text{gs}\rangle$  or  $|\psi_T\rangle$  without increasing its dimension  $\chi$ . If  $A$  contains an arbitrary sum of products of local operators  $a_n$ , one could simply carry out a separate DMRG calculation for each  $e^{iHt}a_n|\text{gs}\rangle$  or  $e^{-iHt+iH_Q t}a_n|\psi_T\rangle$ . This is possible in principle [56] but typically increases the computational effort by a factor of the order of the system size. It can be avoided trivially in case that  $A$  can be expressed in terms of a MPO with a small bond dimension. We will now discuss one instructive example for didactic purposes.

Let us assume that we want to calculate the autocorrelator  $C_T^J(2t)$  of the global spin current  $J = \sum_i j_i$ ,  $j_i = (S_i^+ S_{i+1}^- - S_i^- S_{i+1}^+)/2i$  for the XXZ chain defined in Eq. (8). Spatial translation invariance stipulates  $C_T^J(2t) = L C_T^{j_i/2j}(2t)$ , and in absence of a magnetic field ( $b = 0$ ) spin flip symmetry yields  $C_T^{j_i/2j}(2t) = 2C_T^{j_i/2j\uparrow}(2t)$ , where  $J = J_\uparrow + J_\uparrow^\dagger$ . Instead of computing each term in  $e^{-iHt+iH_Q t}J_\uparrow|\psi_T\rangle$  individually [56], one can express  $J_\uparrow$  in terms of

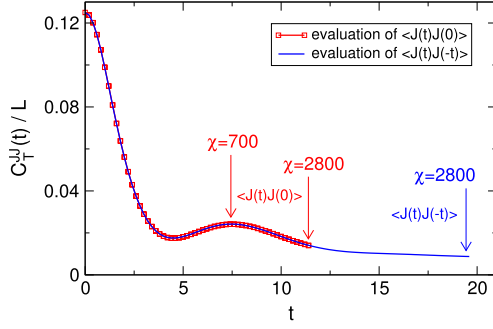


**Fig. 3.** (Color online) Global spin current correlation function of the isotropic XXZ chain ( $\Delta = 1$ ,  $b = 0$ ) at infinite temperature. If one ‘exploits time translation invariance’  $C_T^J(2t) = \text{Tr}[\rho_T J(t)J(-t)]$ , one can access time scales twice as large at virtually no additional effort [34]. The calculation can be carried out efficiently within a MPS based DMRG code (see Section 3.3).

a matrix product operator  $J_\uparrow = \prod_{l=1}^L J_\uparrow^{[l]}$  with

$$J_\uparrow^{[1]} = \begin{pmatrix} 0 & S_1^+ & 0 \\ 0 & \frac{S_1^-}{2i} & 0 \end{pmatrix}, \quad J_\uparrow^{[l=2\dots L-1]} = \begin{pmatrix} 1 & 0 & 0 \\ S_l^- & 0 & 0 \\ 0 & \frac{S_l^+}{2i} & 0 \end{pmatrix}, \quad (23)$$

$$J_\uparrow^{[L]} = \begin{pmatrix} 1 \\ S_L^- \\ 0 \end{pmatrix}.$$

Applying  $J_\uparrow \otimes \mathbb{1}_Q$  to  $|\psi_T\rangle$  yields a new MPS (with a bond dimension increased by a factor of 3), which can then be time evolved via  $e^{-iHt+iHQ t}$ . This altogether illustrates that Eq. (21) can be incorporated readily. An example for how this ‘trick’ allows to reach larger time scales is shown in Fig. 3.

#### 4. The beauty of python

In this section, we illustrate the numerical simplicity of the core DMRG algorithms (thoroughly described in Ref. [2]) if implemented within the python programming language. We hope to advocate the method to colleagues new to its realm and try to stimulate the development of new DMRG codes.

For reasons of completeness, we first briefly recapitulate the idea of singular value decompositions (SVDs), which are the most important ingredient in DMRG calculations. A SVD guarantees that *any* rectangular matrix  $M$  of dimensions  $\chi_1 \times \chi_2$  can be decomposed as

$$M = USV^\dagger, \quad (24)$$

where  $\dim(U) = \chi_1 \times \min(\chi_1, \chi_2)$ ,  $\dim(S) = \min(\chi_1, \chi_2) \times \min(\chi_1, \chi_2)$ , and  $\dim(V^\dagger) = \min(\chi_1, \chi_2) \times \chi_2$ .  $U$  has orthogonal columns and  $V$  has orthogonal rows,  $U^\dagger U = 1$ ,  $V^\dagger V = 1$ . The matrix  $S$  is diagonal, and its entries are called the singular values.

Let us now assume that we want to time evolve a given MPS whose matrices  $M^{\sigma_l}$  are expressed in the ‘ $\Lambda - \Gamma$  form’

$$M_{a_l a_{l+1}}^{\sigma_l} = \Lambda_{a_l}^l \Gamma_{a_l a_{l+1}}^{\sigma_l}. \quad (25)$$

As usual, the local Hilbert space and (position-dependent) bond dimensions are denoted by  $d$  and  $\chi_l$ , respectively. After a Trotter decomposition of  $e^{-iHt}$ , the key task is to apply local operators  $O(\sigma_l, \sigma_{l+1}; \tilde{\sigma}_l, \tilde{\sigma}'_{l+1})$  to Eq. (1). The first step (labeled ‘step 1’ in the python code below) is to form the three-site wave function

$$\Psi^{\sigma_0 \sigma_1} = \Lambda^0 \Gamma^{\sigma_0} \Lambda^1 \Gamma^{\sigma_1} \Lambda^2, \quad (26)$$

where we have randomly set  $l = 0$  to keep the notation simple. Next (step 2), we apply  $O(\sigma_0, \sigma_1; \tilde{\sigma}_0, \tilde{\sigma}_1)$ ,

$$\Phi_{a_0 a_2}^{\sigma_0 \sigma_1} = \sum_{\tilde{\sigma}_0 \tilde{\sigma}_1} O(\sigma_0, \sigma_1; \tilde{\sigma}_0, \tilde{\sigma}_1) \Psi_{a_0 a_2}^{\tilde{\sigma}_0 \tilde{\sigma}_1}, \quad (27)$$

and carry out a singular value decomposition of the appropriately reshaped tensor  $\Phi_{\sigma_0 a_0, \sigma_1 a_2}$  (step 3):

$$\Phi_{\sigma_0 a_0, \sigma_1 a_2} = \sum_{a_1} U_{\sigma_0 a_0, a_1} S_{a_1} V_{a_1, \sigma_1 a_2}. \quad (28)$$

The updated matrices  $\tilde{\Gamma}^{\sigma_0}$ ,  $\tilde{\Lambda}^1$ , and  $\tilde{\Gamma}^{\sigma_1}$  are then obtained as (step 4)

$$\begin{aligned} \tilde{\Gamma}_{a_0, a_1}^{\sigma_0} &= U_{\sigma_0 a_0, a_1} / \Lambda_{a_0}^0, & \tilde{\Lambda}_{a_1}^1 &= S_{a_1}, \\ \tilde{\Gamma}_{a_1, a_2}^{\sigma_1} &= V_{a_1, \sigma_1 a_2} / \Lambda_{a_2}^2, \end{aligned} \quad (29)$$

where we ignore the subtlety of a numerical division by (potentially) small singular values [57]. The bond dimension  $\chi_1$  increased by a factor of  $d$ ; it is usually truncated down to a given  $\chi_{1, \max}$ , and the associated error is controlled by the discarded weight

$$\text{discarded} = \sum_{a_1=\chi_{1, \max}+1}^{d\chi_1} (S_{a_1})^2. \quad (30)$$

The above steps can be implemented straightforwardly within python:

```
import numpy as np

def bond(l0, G0, l1, G1, l2, d, chi_max, O):

    # initial bond dimensions
    chi0=len(G0); chi2=len(G2)

    # step 1: form 3-site tensor
    Psi = np.tensordot( np.diag(l0), G0, axes=(1,1) )
    Psi = np.tensordot( Psi, np.diag(l1), axes=(2,0) )
    Psi = np.tensordot( Psi, G1, axes=(2,1) )
    Psi = np.tensordot( Psi, np.diag(l2), axes=(3,0) )

    # step 2: apply local time evolution operator
    Phi = np.tensordot( Psi, O, axes=([1,2],[0,1]) )
    Phi = np.transpose( Phi, (2,0,3,1) )
    Phi = np.reshape ( Phi, (d*chi0,d*chi2) )

    # step 3: singular value decomposition
    U, S, V = np.linalg.svd(Phi,0)

    # step 4: truncate and reshape
    chi1 = min( len(S), chi_max )

    discarded = np.sum(S[chi1]**2) / np.sum(S**2)
    tilde_l1 = S[0:chi1] / np.sqrt(np.sum(S[0:chi1]**2))

    U = np.reshape ( U[:,0:chi1], (d,chi0,chi1) )
    U = np.tensordot( U, np.diag(1.0/l0), axes=(1,0) )
    tilde_G0 = np.transpose( U, (0,2,1) )

    V = np.reshape ( (V.T)[0:chi1], (d,chi2,chi1) )
    tilde_G1 = np.tensordot( V, np.diag(1.0/l2), axes=(1,0) )

    return tilde_G0, tilde_l1, tilde_G1, discarded
```

where  $\Lambda^l$  and  $\Gamma^l$  are arrays of size  $\chi_l$  and  $(d, \chi_l, \chi_{l+1})$ , respectively. The by far most time consuming parts of this algorithm are matrix multiplications (‘tensordot’) as well as the singular value decomposition, which are elegantly wrapped to lapack routines through the ‘numpy’ package. The numerical overhead due to the inefficiency of python is almost completely negligible. Significant speedups can be achieved (1) by compiling numpy using an efficient and parallelized implementation of lapack (e.g., Intel’s Math Kernel Library), and (2) by carrying out the time evolution on different bonds in

parallel via high-level parallelization in python. A typical run time for a single bond update (i.e., a single call of the above code) of a random initial state under the spin-1/2 Hamiltonian of Eq. (8) using a single node of a standard 2015 cluster (2x Xeon Intel 10-core IvyBridge CPUs running at 2.5 GHz) is 4 s for a bond dimension of  $\chi = 1000$  and 210 s for a bond dimension of  $\chi = 4000$ . The major disadvantage of python is the lack of direct control over the memory resources. Generalizing the above routine to a next-nearest neighbor interaction is extremely straightforward. Abelian symmetries can be incorporated readily and speed up calculations by a factor of  $\sim 10$  for a bond dimension of  $\chi = 1000$  (exploiting continuous symmetries, however, is a challenging task [50–52]).

## 5. Summary

We discussed a few simple tricks to extend the range of time-dependent DMRG simulations. In particular, we illustrated (1) how to ‘combine’ the Schrödinger- and Heisenberg picture in the evaluation of  $\langle \psi | A(t) | \psi \rangle$  as well as for similar quench dynamics at finite temperatures, (2) how to compute  $A(t)$  within a MPS based DMRG code, (3) how to efficiently exploit time translation invariance in linear response correlation functions, and (4) how to analytically understand why a recently-introduced disentangler succeeds in reducing the entanglement growth of calculations at  $T > 0$ . Aiming at beginners, we presented the most important aspects of how to implement these tricks in practice.

## Acknowledgments

We are grateful to Thomas Barthel and Volker Meden for useful suggestions. Support by the Nanostructured Thermoelectrics program of LBNL (CK) is acknowledged.

## References

- [1] U. Schollwöck, *Rev. Modern Phys.* 77 (2005) 259.
- [2] U. Schollwöck, *Ann. Phys.* 326 (2011) 96.
- [3] S.R. White, *Phys. Rev. Lett.* 69 (1992) 2863.
- [4] S.R. White, *Phys. Rev. B* 48 (1993) 10345.
- [5] M. Fannes, B. Nachtergaele, R.F. Werner, *J. Phys. A: Math. Gen.* 24 (1991) L185.
- [6] S. Östlund, S. Rommer, *Phys. Rev. Lett.* 75 (1995) 3537.
- [7] F. Verstraete, J.I. Cirac, V. Murg, *Adv. Phys.* 57 (2008) 143.
- [8] F. Verstraete, J.I. Cirac, *Phys. Rev. B* 73 (2006) 094423.
- [9] N. Schuch, M.M. Wolf, F. Verstraete, J.I. Cirac, *Phys. Rev. Lett.* 100 (2008) 030504.
- [10] J. Eisert, M. Cramer, M.B. Plenio, *Rev. Modern Phys.* 82 (2010) 277.
- [11] T. Prosen, M. Žnidarič, *J. Stat. Mech.* (2009) P02035.
- [12] M.J. Hartmann, J. Prior, S.R. Clark, M.B. Plenio, *Phys. Rev. Lett.* 102 (2009) 057202.
- [13] D. Muth, R.G. Unanyan, M. Fleischhauer, *Phys. Rev. Lett.* 106 (2011) 077202.
- [14] T. Prosen, M. Žnidarič, *Phys. Rev. E* 75 (2007) 015202(R).
- [15] I. Pižorn, T. Prosen, *Phys. Rev. B* 79 (2009) 184416.
- [16] S.R. Clark, J. Prior, M.J. Hartmann, D. Jaksch, M.B. Plenio, *New J. Phys.* 12 (2010) 02500.
- [17] T. Barthel, M. Kliesch, *Phys. Rev. Lett.* 108 (2012) 230504.
- [18] G. Vidal, *Phys. Rev. Lett.* 93 (2004) 040502.
- [19] S.R. White, A.E. Feiguin, *Phys. Rev. Lett.* 93 (2004) 076401.
- [20] A. Daley, C. Kollath, U. Schollwöck, G. Vidal, *J. Stat. Mech.* (2004) P04005.
- [21] S.R. White, A.E. Feiguin, *Phys. Rev. B* 72 (2005) 020404(R).
- [22] P. Schmitteckert, *Phys. Rev. B* 70 (2004) 121302(R).
- [23] G. Vidal, *Phys. Rev. Lett.* 98 (2007) 070201.
- [24] K. Hallberg, *Phys. Rev. B* 52 (1995) 9827(R).
- [25] S. Ramasesha, S.K. Pati, H. Krishnamurthy, Z. Shuai, J. Bredas, *Synth. Met.* 85 (1997) 1019.
- [26] E.D. Kühner, S.R. White, *Phys. Rev. B* 60 (1999) 335.
- [27] E. Jeckelmann, *Phys. Rev. B* 66 (2002) 045114.
- [28] A. Holzner, A. Weichselbaum, I.P. McCulloch, U. Schollwöck, J. von Delft, *Phys. Rev. B* 83 (2011) 195115.
- [29] P.E. Dargel, A. Honecker, R. Peters, R.M. Noack, T. Pruschke, *Phys. Rev. B* 83 (2011) 161104(R).
- [30] J. Haegeman, J.I. Cirac, T.J. Osborne, I. Pižorn, H. Verschelde, F. Verstraete, *Phys. Rev. Lett.* 107 (2011) 070601.
- [31] A.C. Tiegel, S.R. Manmana, Th. Pruschke, A. Honecker, *Phys. Rev. B* 90 (2014) 060406(R).
- [32] M. Suzuki, *Prog. Theor. Phys.* 56 (1976) 1454.
- [33] M.C. Bañuls, M.B. Hastings, F. Verstraete, J.I. Cirac, *Phys. Rev. Lett.* 102 (2009) 240603.
- [34] T. Barthel, *New J. Phys.* 15 (2013) 073010.
- [35] T. Barthel, U. Schollwöck, S. Sachdev, arXiv:1212.3570.
- [36] A. Uhlmann, *Rep. Math. Phys.* 9 (1976) 273; A. Uhlmann, *Rep. Math. Phys.* 24 (1986) 229.
- [37] A.E. Feiguin, S. White, *Phys. Rev. B* 72 (2005) 220401(R).
- [38] T. Barthel, U. Schollwöck, S.R. White, *Phys. Rev. B* 79 (2009) 245101.
- [39] A.E. Feiguin, G.A. Fiete, *Phys. Rev. B* 81 (2010) 075108.
- [40] C. Karrasch, J.H. Bardarson, J.E. Moore, *Phys. Rev. Lett.* 108 (2012) 227206.
- [41] S.R. White, *Phys. Rev. Lett.* 102 (2009) 190601.
- [42] F. Verstraete, J.J. García-Ripoll, J.I. Cirac, *Phys. Rev. Lett.* 93 (2004) 207204.
- [43] M. Zwolak, G. Vidal, *Phys. Rev. Lett.* 93 (2004) 207205.
- [44] X.Q. Wang, T. Xiang, *Phys. Rev. B* 56 (1997) 5061.
- [45] N. Shibata, *J. Phys. Soc. Japan* 66 (1997) 2221.
- [46] J. Sirker, A. Klümper, *Phys. Rev. B* 71 (2005) 241101(R).
- [47] J. Sirker, R.G. Pereira, I. Affleck, *Phys. Rev. Lett.* 103 (2009) 216602.
- [48] D. Muth, *J. Stat. Mech.* (2011) P11020.
- [49] C. Karrasch, J.E. Moore, F. Heidrich-Meisner, *Phys. Rev. B* 89 (2014) 075139.
- [50] I.P. McCulloch, M. Gulácsi, *Europhys. Lett.* 57 (2002) 852.
- [51] I.P. McCulloch, *J. Stat. Mech.* (2007) P10014.
- [52] S. Singh, H.-Q. Zhou, G. Vidal, *New J. Phys.* 12 (2010) 033029.
- [53] C. Karrasch, J.H. Bardarson, J.E. Moore, *New J. Phys.* 15 (2013) 083031.
- [54] T. Arimitsu, H. Umezawa, *Prog. Theor. Phys.* 77 (1) (1987) 32–52.
- [55] S.M. Barnett, B.J. Dalton, *J. Phys. A: Math. Gen.* 20 (1987) 411.
- [56] C. Karrasch, J. Hauschild, S. Langer, F. Heidrich-Meisner, *Phys. Rev. B* 87 (2013) 245128.
- [57] M. Hastings, *J. Math. Phys.* 50 (2009) 095207.